THE PENNSYLVANIA STATE UNIVERSITY
SCHREYER HONORS COLLEGE

DEPARTMENT OF BIOLOGY

GENETIC ANALYSIS OF THE DROSOPHILA ESCRT-III COMPLEX PROTEIN, VPS24, REVEALS REQUIREMENTS IN LYSOSOME HOMEOSTASIS AND AUTOPHAGY

JONATHAN FLORIAN
SPRING 2020

A thesis
submitted in partial fulfillment
of the requirements
for a baccalaureate degree
in Biomedical Engineering
with honors in Biology

Reviewed and approved* by the following:

Fumiko Kawasaki
Associate Research Professor
Thesis Supervisor

Richard Ordway
Professor of Molecular Neuroscience and Genetics
Honors Adviser

* Electronic approvals are on file.

Abstract

The ESCRT (Endosomal Sorting Complexes Required for Transport) pathway is evolutionarily conserved across all eukaryotes and plays key roles in a variety of membrane remodeling processes. A new *Drosophila* mutant recovered in our forward genetic screens mapped to the *vps24* gene encoding a subunit of the ESCRT-III complex. Molecular characterization of the mutation predicted a complete loss of VPS24 function. However, the mutant flies develop to adulthood and thus the consequences of removing VPS24 may be studied in a viable multicellular organism. Flies lacking VPS24 function exhibit locomotor deficits and reduced lifespans. Interestingly, these phenotypes were largely rescued by neuronal expression of wild-type VPS24. Further examination revealed that both neuronal and muscle cells exhibit marked expansion of a ubiquitin-positive lysosomal compartment as well as accumulation of autophagic intermediates. Ultrastructural analysis of the $vps24^{1}$ mutant confirmed these observations and revealed that a major component of the expanded neuronal lysosome compartment exhibited a striking tubular network morphology. The results reported indicate that loss of VPS24 function disrupts lysosome homeostasis, as well as autophagy, and suggest a novel role for ESCRT function in lysosome biogenesis through tubular intermediates. To further define the role of VPS24 in this process, we generated transgenic lines expressing VPS24 with a mutated MIM domain expected to disrupt its ability to associate with intermediates in the pathway. Analysis of these lines may further elucidate the role of the ESCRT pathway in lysophagy and lysosome reformation. These studies provide new insight into the *in vivo* functions of the ESCRT pathway in cellular homeostasis and their potential roles in neurodegenerative diseases characterized by defective ESCRT or lysosome function.

Table of Contents

List of Figures iii

List of Tables iv

Acknowledgements v

Chapter 1 Introduction 1

Neurodegenerative Disease 1
Genetic Analysis of Neural Function in *Drosophila melanogaster* 2
Forward Genetic Screen for New Mutants 2
A New Mutation in a *Drosophila* ESCRT III Gene, *vps24* 4
The ESCRT Pathway – Protein Ubiquitination and Lysosomal Degradation 5

Chapter 2 Materials and Methods 9

Drosophila Fly Strains 9
Behavioral Analysis 9
Analysis of Lifespan 10
Western Blot and Analysis 10
Molecular Cloning (see Chapter 4, Molecular Construction of UAS-EGFP-vps24$^{[MIM]}$) 11
Generation of Transgenic Lines (see also Chapter 4) 11

Chapter 3 Behavioral and Cellular Phenotypes in the *vps24*^{1} Mutant 13

The *vps24*^{1} Mutant Exhibits Locomotor Deficits and Reduced Lifespan at Permissive Temperatures 13
Cellular Phenotypes in the *vps24*^{1} Mutant 14

Chapter 4 Future Studies of VPS24 Structure-Function: Transgenic Expression of an MIM Domain Mutant 20

Domain Structure of VPS24 20
Molecular Construction of UAS-EGFP-vps24$^{[MIM]}$ 21
Generation of Transgenic Lines 24

Chapter 5 Discussion and Future Directions 25

Bibliography 28

List of Figures

Figure 1. A forward genetic screen and recovery of a new temperature-sensitive (TS) paralytic mutant.....3

Figure 2. Rescue of the *vps24*^{1} TS paralytic phenotype by neuronal expression of the wild-type VPS24 protein. 5

Figure 3. The *vps24* gene encodes a component of the ESCRT Pathway. 7

Figure 4. The *vps24*^{1} mutant exhibits locomotor deficits and reduced lifespan.....14

Figure 5. Ubiquitin-positive compartments accumulate in neurons and muscle of the *vps24*^{1} mutant.....15

Figure 6. Ultrastructural analysis of the *vps24*^{1} mutant. 18

Figure 7. Domain structure of VPS24.....21

Figure 8. PCR-based site-specific mutagenesis. 22

Figure 9. Generation of the EGFP-vps24$^{[MIM]}$ transgene construct in the pUAST vector. 23

Figure 10. Analysis of transgenic expression levels of individual EGFP-VPS24$^{[MIM]}$ lines....24

List of Tables

Table 1. *Drosophila* UAS-GAL4 lines used in rescue experiments. 4

Table 2. Primers used to introduce the MIM domain mutation. 22

Acknowledgements

I would like to thank Dr. Fumiko Kawasaki and Dr. Richard Ordway for giving me the opportunity to work in their lab and providing exceptional guidance in research, professional development, and academics. Their dependable support throughout my undergraduate career has taught me the significance of cooperation and perseverance in conducting research.

I am also appreciative of the assistance of former lab members Mackenzie Moon, Jaehee Kim, Linda Guo, and Noelle Loonce, who imparted their knowledge of the lab's protocols to me and expedited my transition to and growth within the lab. I would also like to thank current lab members Samuel DeMatte and Devon Sweeder for their contributions to this work. All of these people have made my work environment welcoming and enjoyable, and their influence has greatly shaped my views of and approach to research moving forward.

Chapter 1

Introduction

Neurodegenerative Disease

Neurodegenerative diseases (NDDs) are characterized by the gradual loss of cognitive and motor function via nervous system cell death (Katsuno, Sahashi, Iguchi, & Hashizume, 2018). Common diseases include Alzheimer's disease, Parkinson's disease, and Huntington's disease, conditions for which no treatment has been established (Cummings, 2017). These disorders have significant effects on the most at-risk population: the elderly. Millions of people around the world currently suffer from NDDs. In addition, projected rises in life expectancies and elderly populations in both developing and developed countries indicate that the prevalence of NDDs will likely increase by 2030 (Taylor, Brown, & Cleveland, 2016; Veron, Kinsella, & Velkoff, 2002).

Despite a large variety of identified neurodegenerative diseases, a symptom universally observed is the failure of cellular proteostasis (Katsuno et al., 2018). Normally, abnormal and misfolded proteins are cleared before they can accumulate and increase cell proteotoxicity (Lim & Yue, 2015). Neurons are intrinsically less competent in maintaining proteostasis relative to other cell types, although the reasons for this are still unknown (Katsuno et al., 2018). Dysfunctional faulty protein removal mechanisms associated with neurodegenerative disorders result in the formation of toxic aggregates; as such, inhibition of protein accumulation has been a proposed method of slowing NDD progression.

Genetic Analysis of Neural Function in *Drosophila melanogaster*

Our laboratory has employed a *Drosophila melanogaster* model, which exhibits powerful genetic tools. Its genetic capabilities includes, but is not limited to, simple, rapid mutagenesis as well as temporal and tissue-specific transgene expression (Jeibmann & Paulus, 2009; Pandey & Nichols, 2011). In addition, numerous neurological and physiological properties and pathways of fruit flies are conserved with mammals. For instance, 75% of disease-causing genes in humans are believed to exist in *Drosophila* as well (Lloyd & Taylor, 2010; Reiter, Potocki, Chien, Gribskov, & Bier, 2001). Our previous studies have utilized adult Dorsal Longitudinal Muscle (DLM) neuromuscular synapses, tripartite synapses exhibiting structural and functional properties similar to those of their mammalian counterparts, in a model for environmental stress-induced failure of proteostasis and degeneration (Danjo, Kawasaki, & Ordway, 2011; Kawasaki et al., 2016).

Of particular significance to our lab are mutations causing temperature-sensitive (TS) neural dysfunction. This approach allows for selective activation of the mutant phenotype and the examination of essential processes required for survival. By raising the flies under the nonpermissive temperature and inducing the phenotype at a given time, the mutations can be studied at any developmental stage. In addition, comparisons can be made between flies in the same line before and after the protein is rendered nonfunctional.

Forward Genetic Screen for New Mutants

Our previous work has involved genetic analysis of TS paralytic mutants to examine the molecular mechanisms of chemical synaptic transmission (Brooks, Felling, Kawasaki, &

Ordway, 2003; Kawasaki, Collins, & Ordway, 2002; Kawasaki et al., 2016; Kawasaki & Ordway, 2009; Wu, Kawasaki, & Ordway, 2005; W. Yu, Kawasaki, & Ordway, 2011). As an extension of this approach, the current study initiated a forward genetic screen for TS paralytic alleles of candidate genes implicated in synaptic function (Figure 1A). A new mutant exhibited a recessive TS paralytic phenotype (Figure 1B) and, despite not mapping to any of the candidate genes, was mapped to a gene removed by the Df(3R)Exel6140 deficiency. Complementation testing using existing mutations occurring within this deficiency region revealed that the mutant is allelic to the *vps24* gene, which encodes a subunit of the ESCRT-III complex.

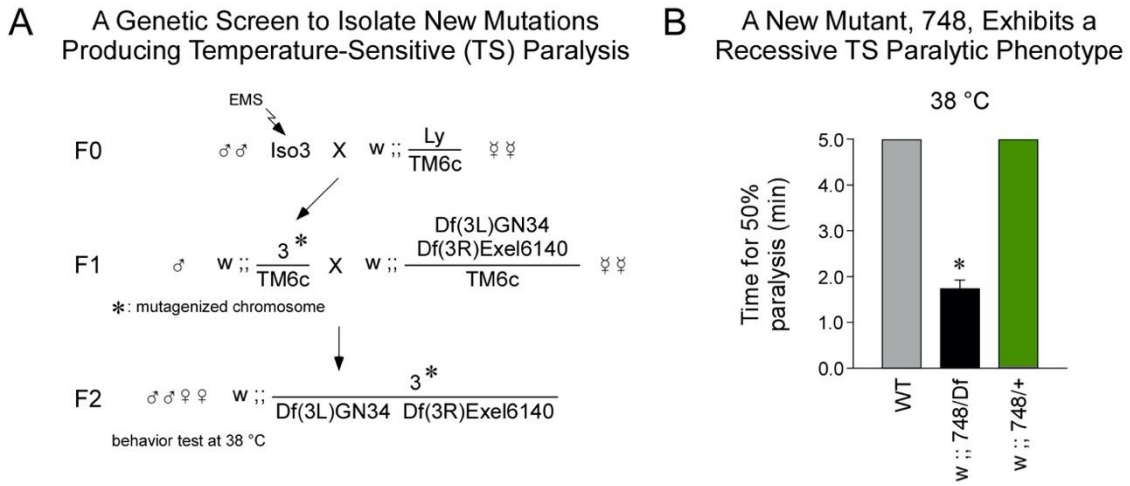

Figure 1. A forward genetic screen and recovery of a new temperature-sensitive (TS) paralytic mutant.

(A) Male flies with an isogenized third chromosome (Iso3) were exposed to ethyl methane sulphonate (EMS). Mutagenized males were mated with females carrying the third chromosome marker *Lyra* (*Ly*), *in trans* to a balancer chromosome *TM6c*. F1 males carrying a mutagenized third chromosome (3*) *in trans* to *TM6c* were crossed to females with the third chromosome deficiencies *Df(3L)GN34* and *Df(3R)Exel6140*. F2 progeny carrying 3* *in trans* to the deficiency chromosome were screened for motor defects at 38°C. (B) *748/Df(3R)Exel6140* flies (748/Df) exhibit rapid paralysis at 38°C, whereas wild-type flies (WT) do not. Tests of *748/+* flies indicated the phenotype is recessive. Tests were truncated at 5 minutes if 50% paralysis had not occurred. Error bars indicate SEM and asterisks mark significant differences from control values ($p \leq 0.05$).

A New Mutation in a *Drosophila* ESCRT III Gene, *vps24*

Sequence analysis of genomic DNA from the mutant, now designated as *vps24*^{1}, identified an 11bp deletion from the second bp of the first intron of the *vps24* gene. PCR and sequence analysis of cDNAs between *vps24*^{1} and WT revealed that the mutant exhibited disrupted splicing of the first intron. PCR product sequencing showed this occurred via complete splicing failure, in which the 121bp intronic sequence between Exons 1 and 2 remained, and cryptic splicing, in which an additional splice occurred 20bp upstream of the first intron. Both cases resulted in a truncated VPS24 protein, indicating that the *vps24*^{1} mutant is likely to produce a complete loss of VPS24 function.

The behavioral phenotype of *vps24*^{1} mutants was confirmed through transformation rescue experiments. These studies used the GAL4/UAS system which permits spatial and temporal control of transgene expression (Brand & Perrimon, 1993). To do so, transgenic lines were first established expressing wild-type VPS24 fused with green fluorescent protein (GFP) at its N-terminus. Stocks expressing the transgene in neurons, glia, and muscle in the mutant background were created for further experimentation (Table 1).

Table 1. *Drosophila* UAS-GAL4 lines used in rescue experiments.

Genotype	Site of Expression
w Appl-Gal4/w ; UAS-EGFP-vps24/+ ; vps24^{1}/Df(3R)Exel6140	Neuron
w Mhc-Gal4/w ; UAS-EGFP-vps24/+; vps24^{1}/Df(3R)Exel6140	Muscle
w ; UAS-EGFP-vps24/+ ; Repo-GAL4 vps24^{1}/Df(3R)Exel6140	Glia

In the *vps24*^{1} mutant background, the TS paralytic phenotype was rescued from neural expression of UAS-EGFP-vps24 (Figure 2). Expression of the same transgene with MHC- and

Repo- GAL4 drivers failed to rescue the phenotype, signifying that TS paralysis results from loss of VPS24 function in neurons and not loss of function in muscle or glia.

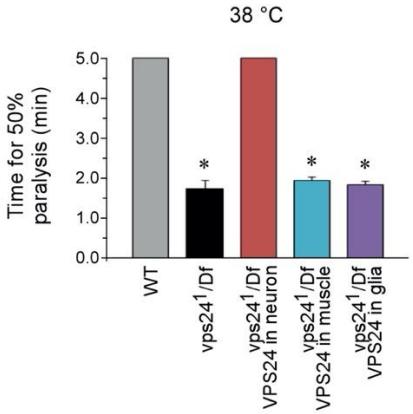

Figure 2. Rescue of the *vps24¹* TS paralytic phenotype by neuronal expression of the wild-type VPS24 protein.

The TS paralytic phenotype of the *vps24¹* mutant was rescued by expression of the wild-type EGFP-VPS24 in neurons but not in muscle or glia. The GAL4 drivers for neuronal, muscle, and glial expression were *Appl-Gal4, MHC-GAL4, and Repo-GAL4,* respectively.

Since the initial genetic screen was for synaptic transmission mutants, a secondary screen was conducted to determine whether TS paralysis results from a defect in synaptic function. For this purpose, electrophysiological studies were performed at adult neuromuscular synapses of the flight motor as described previously (Kawasaki, Mattiuz, & Ordway, 1998). DLM neuromuscular synapse function was normal in the *vps24¹* mutant with respect to short-term plasticity and the amplitude and waveform of individual EPSCs. Therefore, studies of synaptic transmission were not pursued further in this mutant.

The ESCRT Pathway – Protein Ubiquitination and Lysosomal Degradation

The primary process of preventing toxic protein accumulation is the highly conserved lysosomal degradation pathway (Clague & Urbé, 2010). One method of disposal in a majority of

cell types relies on late endosomes known as multivesicular bodies (MVBs) (Fader & Colombo, 2009). The process begins when faulty proteins leading to proteotoxicity are labeled with ubiquitin via an E1-E2-E3 enzyme ubiquitin thioester cascade (Scheffner, Nuber, & Huibregtse, 1995). Through endocytosis, the monoubiquitinated surface proteins and ligands are internalized to the surface of early endosomes (Figure 3A). MVBs are formed from the early endosomes and possess ubiquitin-targeted proteins along intraluminal vesicle membranes. Although the multivesicular bodies may interact with other components of the endocytic pathway, MVBs can fuse with lysosomes alone. Hydrolytic components inside the lysosome then degrade the MVB components. This process is closely related to the second and most common method of lysosomal degradation: autophagy. To traffic long-lived proteins, macromolecules, and organelles within the cell, the surrounding cytoplasm is enclosed in a phagophore that forms a double-membrane autophagosome. The monoubiquitin or ubiquitin chains on the cargo bind to P62 filaments, adaptors linking them to ATG8 proteins on the membrane during autophagosome formation, to ensure they remain in the lumen (Danieli & Martens, 2018; Weidberg, Shvets, & Elazar, 2011). Fusion with the MVB or other endocytic pathway components, if it occurs, creates a hybrid organelle termed the amphisome (Fader & Colombo, 2009). Subsequent fusion of the autophagosome or amphisome with the lysosome yields digested intraluminal components.

The ESCRT pathway is evolutionarily conserved from yeast to mammals and functions in membrane remodeling, a process essential for multivesicular body formation and autophagy (Figure 3A) (Henne, Buchkovich, & Emr, 2011; Leung, Dacks, & Field, 2008). It is comprised of five complexes: ESCRT-0, ESCRT-I, ESCRT-II, ESCRT-III (subunit and complex), and Vps4-Vta1. ESCRT-0 initiates the pathway by associating with ubiquitinated cargo at the plasma membrane (Figure 3B). While the membrane invaginates and forms early endosomes,

the ESCRT-I and ESCRT-II complexes are recruited by ubiquitin to bind together and localize the cargo. ESCRT-II nucleates ESCRT-III subunits, which form a complex, recruit deubiquitinating machinery, and facilitate vesicle maturation and neck constriction. Following vesicle scission, the Vps4-Vta1 complex disassociates the ESCRT-III complex, leaving the cargo within the mature vesicle plasma membrane. A nonfunctional ESCRT-III protein is therefore expected to inhibit membrane pinching in MVB biogenesis and autophagy and subsequently hamper proteostasis.

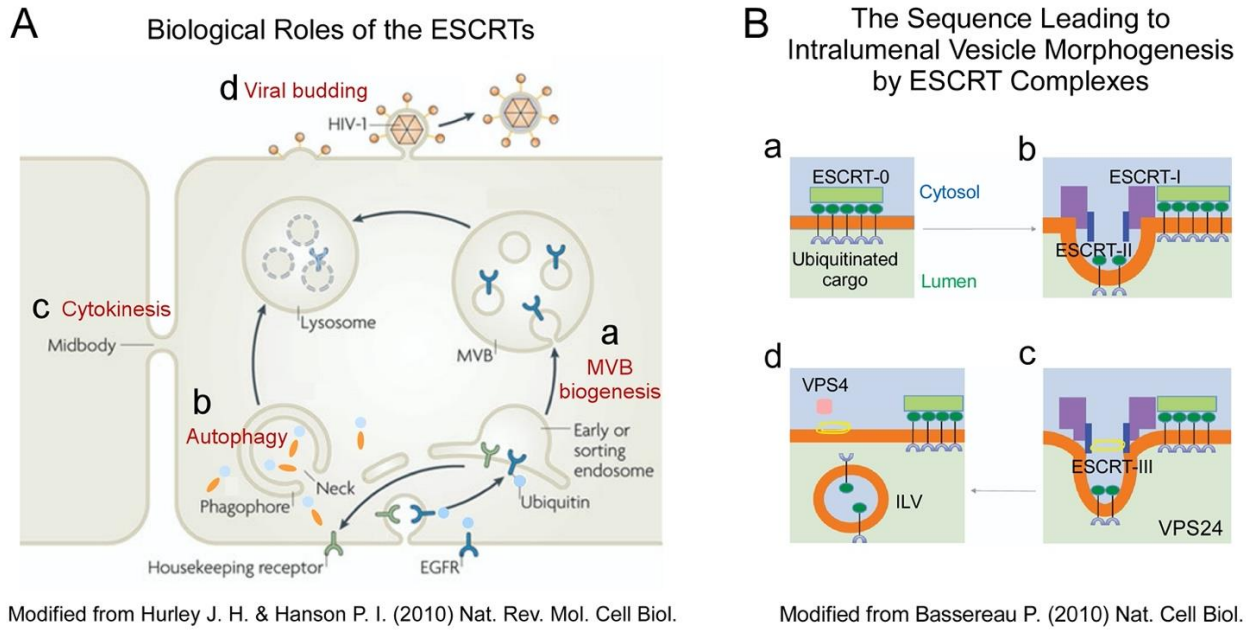

Figure 3. The *vps24* gene encodes a component of the ESCRT Pathway.

(A) Multivesicular body (MVB) biogenesis (a) and autophagy (b) require all of the ESCRTs. In contrast, cytokinesis (c) and HI-V1 budding (d) require only ESCRT-I and ESCRT-III. (B) (a) ESCRT-0 clusters ubiquitinated cargoes. (b) ESCRT-I and ESCRT-II together form membrane invaginations and are localized inside the bud neck. Cargoes are sequestered in the bud. (c) ESCRT-III assembles at the neck of the bud, colocalizing with ESCRT-I and -II. (d) Vesicle scission by ESCRT-III leading to the formation of ILV. The ATPase VPS4 is recruited to dissociate ESCRT-III oligomers.

Autophagy deregulations due to insufficient pathway activation, reduced lysosomal function, and pathological pathway activation are known to induce proteinopathies in

neurodegenerative diseases. Such observations necessitate an examination of the molecular mechanisms underlying lysosomal autophagic dysfunction. A better understanding of defective protein degradation is required for the design of NDD treatments.

Chapter 2

Materials and Methods

Drosophila Fly Strains

Wild-type flies, *Canton-S*, as well as *Appl-GAL4*, *w;;Ly/TM6c* and *UAS-EGFP-vps24* were from our laboratory stock collection. *Mhc-Gal4*, *Repo-Gal4*, *UAS-GFP* and *UAS-GFP-mCherry-atg8a*, *Df(3L)GN34* and *Df(3R)Exel6140* were obtained from the Bloomington Stock Center (Indiana University, Bloomington, IN). *UAS-EGFP-vps24*[MIM] transgenic lines were generated in the current study (see "Generation of Transgenic Lines" and Chapter 4). *UAS-GFP-LAMP* (Pulipparacharuvil et al., 2005), *UAS-cathB-3XmCherry* (Csizmadia et al., 2018) transgenic lines were kindly provided by Dr. Helmut Krämer (University of Texas Southwestern Medical Center, Dallas, TX) and Dr. Gábor Juhász (Eötvös Loránd University, Hungary), respectively. Stocks and crosses were cultured on a conventional cornmeal-molasses-yeast medium at 20°C in a 12-hour day-night cycle. All experiments were carried out using virgin female flies.

Behavioral Analysis

To examine the paralytic phenotype, as well as its rescue, six 7d old female flies of each line were transferred to vials. After placing the vials in a 38°C water bath, the time it took to reach 50% paralysis was recorded. Tests were truncated to 5 minutes if no paralysis occurred.

A climbing test was done to evaluate potential locomotor deficits in the mutant. *vps24*^{1} flies and lines expressing wild-type VPS24 in neurons, glia, and muscle (Table 1) in the mutant

background were established and examined. Six 7d old female flies in each test were transferred to a plugged graduated cylinder. After knocking the flies to the bottom through tapping, the time it took for half of them to climb to the 40ml mark was recorded. If flying was observed in that timeframe, the flies were knocked to the bottom again and the time was reset. Tests were truncated to 2 minutes if 50% climbing had not occurred and 0 was given for the climbing index. Ten samples for each group were tested, and average times were normalized and inverted for climbing index values.

Analysis of Lifespan

Using the same lines, 50 flies of each group were reared in a 20°C refrigerator. Every two days the survivors were transferred to a new vial and the number of deaths were recorded. The test continued until all flies died. Lifespan was assessed at each time point as a percentage of survivors.

Western Blot and Analysis

Western blotting was employed to confirm the expression of UAS-EGFP-VPS24 in the *Drosophila* transgenic lines generated. Five fly heads were homogenized in 100 μl of SDS buffer. 0.5 heads of each line and a Bio-Rad Dual Color Standard were loaded into a 9% polyacrylamide gel and run at 15 mA. The proteins were then transferred to a nitrocellulose membrane at 14V overnight. The membrane was washed with α-GFP (1:500) primary antibody and α-mouse IgG (1:5000) secondary antibody. The loading control was detected by incubating

the membrane with α-ACTIN (1:100) primary antibody. A LI-COR Odyssey CLx system was used to image the membrane, and the images were analyzed using LI-COR Image Studio software. Transgene expression (GFP/ACTIN) for each line were calculated. A molecular weight (log MW in kDa) vs. distance travelled (mm) trendline was created using the size standard and used to determine the MW of each EGFP-VPS24 band.

Molecular Cloning (see Chapter 4, Molecular Construction of UAS-EGFP-vps24$^{[MIM]}$)

To construct the EGFP-vps24$^{[MIM]}$ mutant (R217D L218D) transgene, the R217D L218D mutations were generated by PCR site-directed mutagenesis and incorporated into an EGFP-vps24 construct in pBluescriptI SK-. The resulting EGFP-vps24$^{[MIM]}$ sequence was shuttled into the P element transformation vector, pUAST (Brand & Perrimon, 1993), for generation of transgenic lines.

Generation of Transgenic Lines (see also Chapter 4)

An injection mixture consisting of 60 μl water, 25 μl of EGFP-vps24$^{[MIM]}$ mutant in pUAST (~2.6 μg/μl), 5 μl of helper plasmid (~4.5 μg/μl), and 10 μl of green dye was distributed into microinjection glass capillary needles. Every 30 minutes, embryos from a white-eyed fly stock were collected and arranged onto a glass slide. Under a microscope, micromanipulators and a pressurized syringe were used to inject the solution from the needles to the embryos' posterior region. Embryos were then grown on cornmeal-molasses-yeast medium and transferred to a vial during the larval developmental stage. Subsequent crosses identified lines

with successful integration, revealed the chromosome on which they occurred, and stabilized the mutated chromosome over a balancer chromosome.

Chapter 3

Behavioral and Cellular Phenotypes in the *vps24*^{1} Mutant

The findings discussed in Chapters 3 and 4 are the result of collaborative research efforts in our lab. Other members whose work contributed to this thesis include Samuel DeMatte and Devon Sweeder. I performed experiments in genetics, behavioral analysis, molecular biology, transgenic fly generation, and Western blotting. Immunocytochemistry (ICC), confocal microscopy, and transmission electron microscopy (TEM) were performed by Dr. Fumiko Kawasaki.

The *vps24*^{1} Mutant Exhibits Locomotor Deficits and Reduced Lifespan at Permissive Temperatures

Although *vps24*^{1} mutant flies reach the adult stage with no obvious developmental defects, they display impaired locomotor function even at temperatures permissive for TS paralysis. The mutant flies displayed a significant decline in climbing performance at 7 days of age (Figure 4A), indicating that VPS24 is required for normal locomotor activity. In addition, loss of VPS24 function produces a marked reduction in lifespan to a range of approximately 3-8 weeks (Figure 4B). Notably, both the locomotor and lifespan deficits of the *vps24*^{1} mutant, like the TS paralytic phenotype, are rescued by neuronal expression of wild-type VPS24 but not by expression of this transgene in glia or muscle (Figure 4). The preceding findings reveal that VPS24 function in neurons is critical for basic motor function and viability, consistent with previous studies implicating ESCRT-III components in neurodegenerative disease.

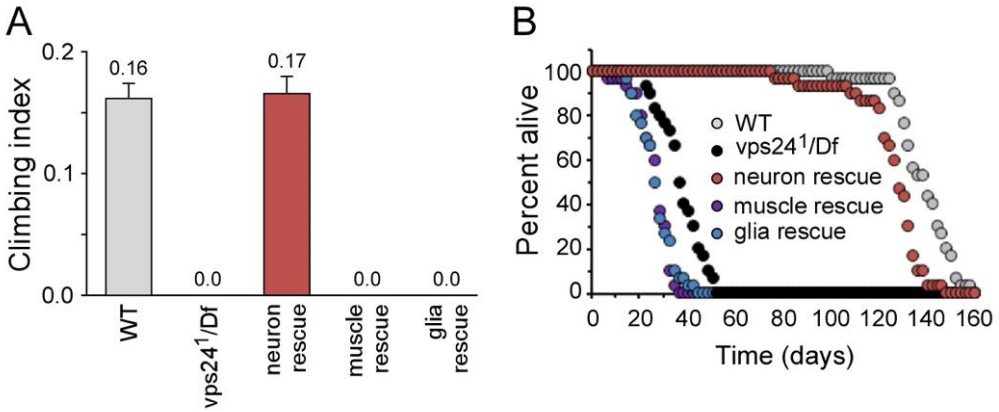

Figure 4. The *vps24¹* mutant exhibits locomotor deficits and reduced lifespan.

(A) Climbing tests indicated no detectable climbing ability in the *vps24¹* mutant. The climbing tests were truncated at 2 min. if 50% climbing had not occurred and zero was given for the climbing index. (B) Loss of the VPS24 function reduced lifespan with respect to WT. These mutant phenotypes were rescued by expression of wild-type EGFP-VPS24 in neurons but not in muscle or glia. In climbing tests, 7d old female flies were examined. Expression of a UAS-EGFP-vps24 transgene was achieved using specific GAL4 drivers for neurons (*Appl-GAL4*), muscle (*MHC-GAL4*), and glia (*Repo-GAL4*). The same GAL4 drivers were used for subsequent cell-type specific expression studies.

Cellular Phenotypes in the *vps24¹* Mutant

Investigation of cellular defects in the *vps24¹* mutant was carried out mainly through ICC and TEM. Key findings from these studies are summarized in this section. Given the established roles of ESCRT function in membrane remodeling and protein degradation, immunocytochemical studies were performed to determine whether the *vps24¹* mutant exhibited altered proteostasis. Initial studies examined the distribution of ubiquitinated proteins in thoracic tissues involved in motor activity, including the thoracic ganglion of the CNS and the three cell types comprising tripartite Dorsal Longitudinal Muscle (DLM) neuromuscular synapses. The mutant exhibited a striking accumulation of ubiquitin-positive structures in both the CNS and DLM flight muscle (Figure 5). Further examination of the CNS using cell type-specific markers

for neurons and glia demonstrated that ubiquitin-positive structures were restricted to neurons and lacking in CNS glia.

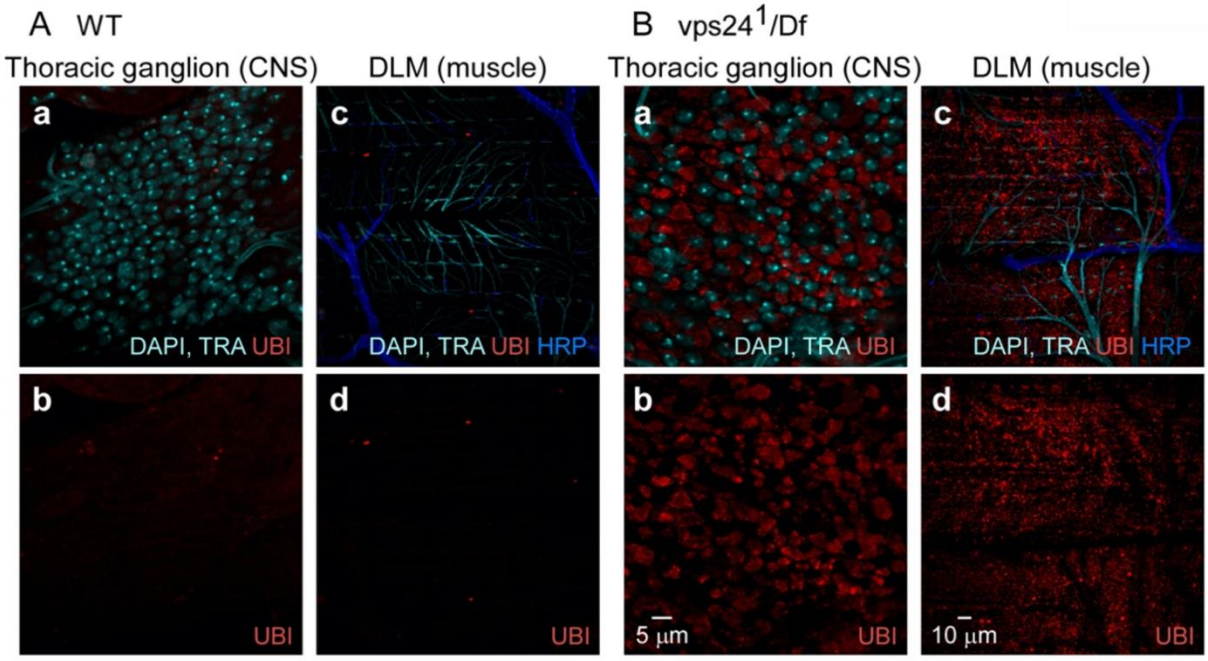

Figure 5. Ubiquitin-positive compartments accumulate in neurons and muscle of the *vps24¹* mutant.

Confocal immunofluorescence images from wild-type (WT) (A) or *vps24[1]/Df(3R)Exel6140* (vps24[1]/Df) mutant flies (B). Ubiquitin (UBI) staining indicates that the *vps24¹* mutant exhibits a marked increase in ubiquitin-positive compartments in CNS (a, b) and muscle (c, d) with respect to WT. DAPI labeling of nuclei and autofluorescence from trachea (TRA) appear in the same channel.

The preceding cellular phenotypes in the CNS neurons and DLM resulted from loss of VPS24 function. This was confirmed by rescue experiments analogous to those performed in the behavior and lifespan studies. Neuronal expression of wild-type VPS24 produced clear rescue of the neuronal phenotype, consistent with the observation that ubiquitin-positive structures were

restricted to neurons. Similarly, the DLM phenotype was rescued by expression of the same transgene in muscle.

Given the known function of VPS24 as a component of the ESCRT pathway, it was of interest to determine whether the *vps24*^{1} mutant phenotype includes an altered distribution of ESCRT proteins. This was achieved through immunocytochemical studies of the endogenous VPS28 protein in the *vps24*^{1} mutant. VPS28 is a component of the ESCRT-I complex that can interact with ESCRT-III components including VPS24. In the wild-type, VPS28 exhibited a diffuse distribution in both the CNS and DLM. In contrast, the VPS28 distribution is altered dramatically in the *vps24*^{1} mutant and is strongly associated with the accumulated ubiquitin-positive structures in both neurons and muscle. These observations suggest that the cellular *vps24*^{1} mutant phenotype involves disruption of ESCRT pathway function leading to aberrant homeostasis in neurons and muscle.

Further characterization of the ubiquitin-positive structures observed in *vps24*^{1} mutant neurons and muscle revealed clear colocalization with two different lysosomal markers, the lysosome-associated membrane protein (LAMP) (Pulipparacharuvil et al., 2005; Rohrer, Schweizer, Russell, & Kornfeld, 1996; Saftig & Klumperman, 2009) and the lysosomal enzyme, Cathepsin B (Csizmadia et al., 2018; Stoka, Turk, & Turk, 2016). These findings indicate that the *vps24*^{1} mutant exhibits an expanded lysosomal compartment highly enriched in ubiquitinated proteins.

VPS24 and the ESCRT pathway are known to participate in autophagic degradation mechanisms (Filimonenko et al., 2007; S. Yu & Melia, 2017) that may include lysophagy (Hung, Chen, Yang, & Yuan Yang, 2013; Papadopoulos & Meyer, 2017). To investigate whether autophagy is disrupted in the *vps24*^{1} mutant, immunocytochemistry studies were carried out

using markers for autophagic intermediates. The P62 protein plays a key role in autophagy as an adaptor between ubiquitinated proteins and the ATG8a protein associated with nascent autophagophores (Pankiv et al., 2007). P62 accumulation is typically interpreted as a disruption of autophagy and accumulation of autophagic intermediates (Bjørkøy et al., 2005; Filimonenko et al., 2007; Gal, Ström, Kilty, Zhang, & Zhu, 2007). Examination of CNS neurons and DLMs of the *vps24*^{1} mutant revealed marked accumulation of endogenous P62 and its colocalization with the ubiquitinated lysosomal compartment.

The preceding findings predict that ultrastructural analysis of the *vps24*^{1} mutant phenotype in CNS neurons and DLM flight muscle should reveal an expanded lysosome compartment as well as accumulation of autophagic intermediates. These cell types were examined by TEM and found to exhibit striking ultrastructural phenotypes suggesting disruption of lysosome homeostasis and autophagy (Figure 6). Neuronal cell bodies, which are surrounded by a thin layer of cytoplasm in wild-type, were dramatically enlarged in the *vps24*^{1} mutant and filled with an expanded, electron-dense membrane compartment (Figure 6A). Features of this compartment included a highly electron-dense population of spherical structures identifiable as autolysosomes (Nagy, Varga, Kovács, Takáts, & Juhász, 2015; Takáts et al., 2014; Tong et al., 2012) as well as a striking tubular network that appeared continuous with some autolysosomes. The distribution of autolysosomes and this tubular network throughout the enlarged cell body is consistent with immunocytochemical studies showing the cell body largely occupied by a ubiquitinated lysosome compartment. The spherical autolysosome-like structures connected to the tubular network were less electron dense than those that appeared to be separate from it, raising the possibility that this tubular network is related to tubular intermediates in lysosome biogenesis (Chen & Yu, 2018; Saffi & Botelho, 2019; L. Yu et al., 2010). In muscle (Figure

6B), accumulation of autolysosomes occurred near the plasma membrane in the *vps24*^{1} mutant. However, the tubular network was not observed. Finally, autophagic intermediates were present in both CNS neurons and DLM flight muscle of the *vps24*^{1} mutant, but not in the wildtype. As described previously (Nagy et al., 2015; Takáts et al., 2014), autophagophore or autophagosome intermediates exhibited a characteristic cleft between membrane sheets. The presence of these autophagic intermediates suggests moderate disruption of autophagy in the *vps24*^{1} mutant.

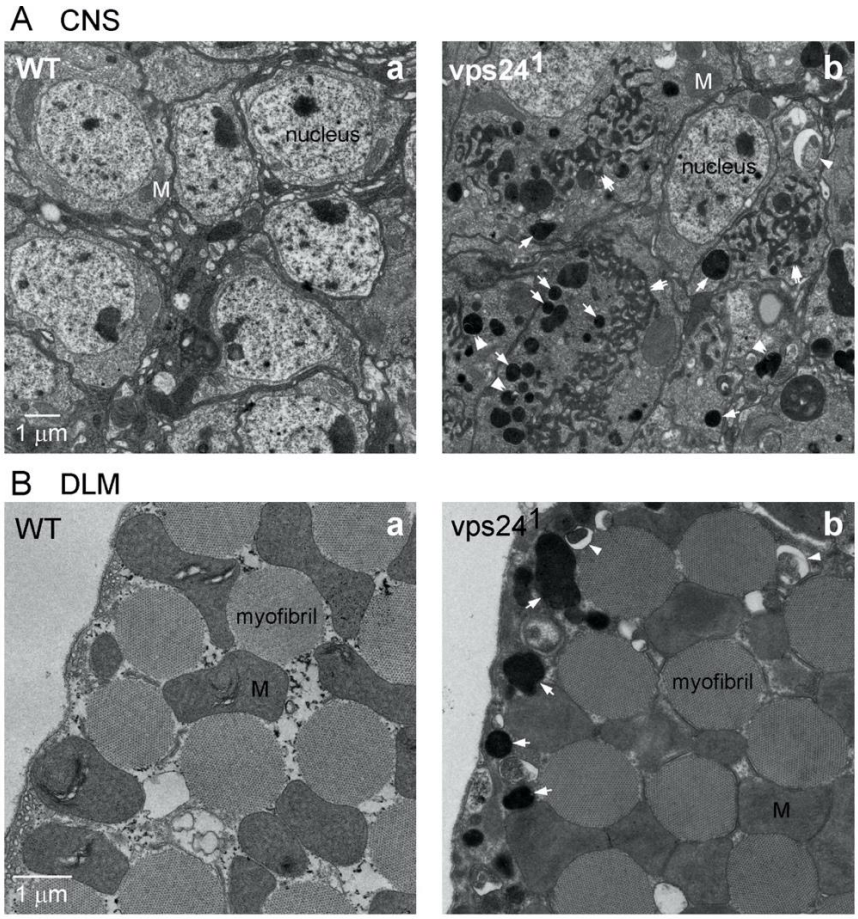

Figure 6. Ultrastructural analysis of the *vps24*^{1} mutant.

Transmission electron microscopy images of CNS neurons (A) and DLM (B) from WT (a) or the *vps24*^{1} mutant (b). In the *vps24*^{1} mutant, accumulation of autolysosomes (arrows) and tubular lysosome structures (double arrows) as well as autophagosomes (arrowheads) are visible, whereas these structures are absent in WT. Extensive tubulation of lysosomal compartments is prominent in the neuron of the mutant. In the muscle of the mutant, mitochondria appear to be swollen.

These ultrastructural studies confirm that loss of VPS24 function results in expansion of the lysosomal compartment and disruption of autophagy. An expanded lysosome compartment has not been described previously in ESCRT pathway mutants. Accumulation of a tubular lysosomal network may be related to tubular intermediate structures in lysosome biogenesis and suggest a novel role for the ESCRT pathway in lysosome homeostasis.

Chapter 4

Future Studies of VPS24 Structure-Function: Transgenic Expression of an MIM Domain Mutant

Domain Structure of VPS24

The VPS24 protein consists of five helical domains (Bajorek et al., 2009; Muzioł et al., 2006) (Figure 7). α1 and α2 are joined into a long hairpin structure that associates with α3 and α4 to form a four-helical bundle. Following the fourth helix is a long loop connecting it to a final helix oriented perpendicular to the bundle. The N-terminus region of VPS24 is positively charged, while the C-terminus region is negatively charged (Shim, Kimpler, & Hanson, 2007). After the α5 helix, the VPS24 protein possesses a Microtubule and transport (MIT)-Interacting Motif (MIM) domain, which is important in forming associations with MIT-domain-containing proteins (Figure 7). Previous works have demonstrated that deletions within the C-terminus of the protein results in ubiquitin accumulation in intracellular compartments (Shim et al., 2007), similar to observations made with the *vps24*^{1} mutant identified here.

Previous studies have shown that two amino acids at positions 0 and +1 within yeast and human MIM domains, Arginine and Leucine, have a role in binding to MIT domains (McCullough, Frost, & Sundquist, 2018; Obita et al., 2007; Stuchell-Brereton et al., 2007). Another group demonstrated in *Aspergillus nidulans* that these same amino acids of the MIM domain are essential for proper VPS24 binding to the effector protein PalB (Rodríguez-Galán, Galindo, Hervás-Aguilar, Arst, & Peñalva, 2009). This structure is conserved between not only these three organisms but also mice, *Drosophila*, *C. elegans*, and *S. cerevisiae* (Figure 7).

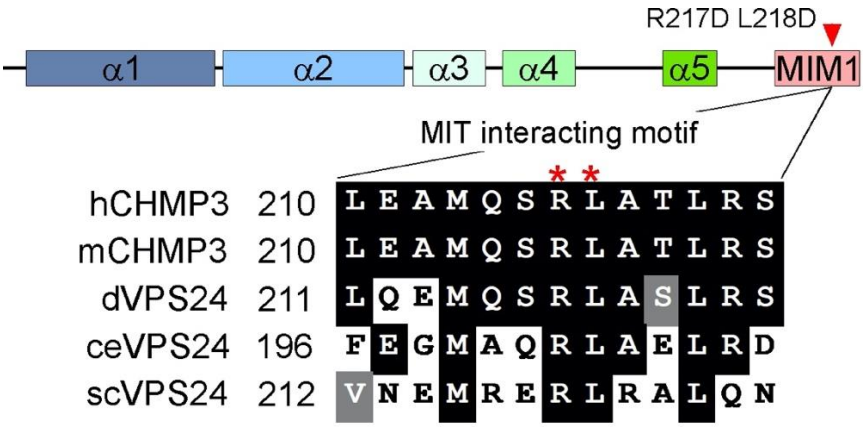

Figure 7. Domain structure of VPS24.

Microtubule-interacting and transport (MIT)-interacting motif 1 (MIM1) domain present in the VPS24 carboxy-terminal mediates binding interactions with MIT domain-containing proteins. Mutations that disrupt MIT binding (R217D L218D) are indicated by the red arrowhead. These mutations were introduced into the *Drosophila* EGFP-VPS24$^{[MIM]}$ transgene. Alignment of VPS24 from human, mouse, *Drosophila*, *C. elegans*, and *S. cerevisiae*. Amino acids changed in the mutant are marked with asterisks. Amino acid identities (black) and similarities (gray) are shaded.

Molecular Construction of UAS-EGFP-vps24$^{[MIM]}$

In *Drosophila* VPS24, adjacent Arg and Leu residues are located at positions 217 and 218 of the MIM1 domain. The aforementioned study using *A. nidulans* generated a mutant form of VPS24 by substituting these two amino acids with Aspartic Acid. This mutation disrupted binding to an effector protein. Our lab is interested in the transgenic expression of a similar R217D L218D mutation in the *Drosophila* VPS24 MIM1 domain to permit identification of lysosome biogenesis pathway intermediates.

To construct the EGFP-vps24$^{[MIM]}$ mutant (R217D L218D) transgene, PCR site-directed mutagenesis via overlap extension (Ho, Hunt, Horton, Pullen, & Pease, 1989) was utilized (Figure 8).

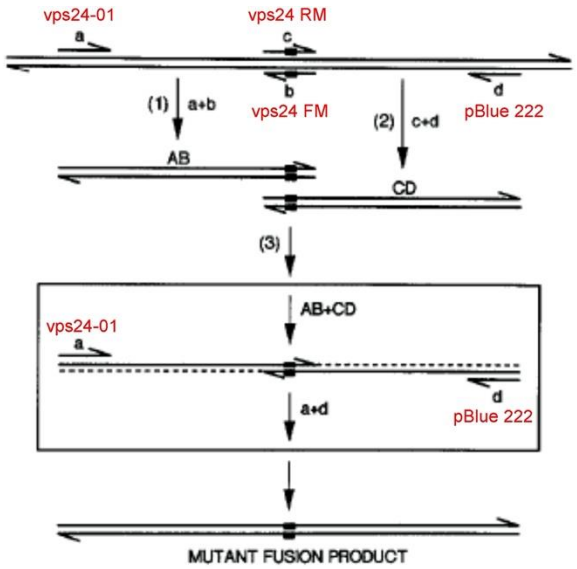

modified from Ho, SN *et al.* (1989) Gene.

Figure 8. PCR-based site-specific mutagenesis.

Primers are represented at their annealing sites on the ds DNA template. Arrows indicate the 5' to 3' orientation. Primer names correspond to those in Table 2. Primers *b* and *c* were designed such that the desired mutation nucleotide sequence is flanked by the WT sequence. The mutant sequence is denoted with small rectangles. (1) The 1st PCR with primers *a* and *b* using WT DNA template yields PCR product AB. (2) The 2nd PCR with primers *c* and *d* using WT DNA template yields PCR product CD. (3) In the 3rd PCR, the denatured PCR products, AB and CD, anneal at the overlap and are extended 3' by DNA polymerase (dotted line) to form the mutant fragments (AB+CD). The mutant fragments are further amplified by PCR with primers *a* and *d*.

The first PCR reaction used EGFP-vps24 in pBluescriptI SK- as the template and the vps24-01 and vps24 FM primers designed by our lab (Table 2). The second reaction used the same template, although the primers were pBlue 222 and a designed vps24 RM (Table 2).

Table 2. Primers used to introduce the MIM domain mutation.

Name	Nucleotide Sequence
vps24-01	atgggcttattcggcaga
vps24 FM	gcagcgaggcGTCATCgctttgcatctc
vps24 RM	gatgcaaagcGATGACgcctcgctgcga
pBlue 222	tagggtgatggttcacgtag

Capital letters indicate substituted nucleotides to introduce the R217D L218D mutations.

Following purification, both products were quantified and incorporated as the DNA template in a third PCR using primers vps24-01 and pBlue 222. Both the mutant PCR product and EGFP-vps24 in pBluscriptI SK- were digested in 60 µl reactions using BssH II and Kpn I restriction enzymes (Figure 9A). The mutated 83 bp insert and pBluescriptI SK- vector were extracted and ligated together. *E. coli* were transformed with the plasmid and individual colonies were cultured. After mini prep extraction, additional 60 µl digestions of EGFP-vps24[MIM] mutant in pBlue and halo K73T in pUAST transformation vector using Not I and Kpn I restriction enzymes were done. As shown in Figure 9B, the desired fragments were isolated and ligated together such that an EGFP-vps24[MIM] mutant in pUAST plasmid was constructed.

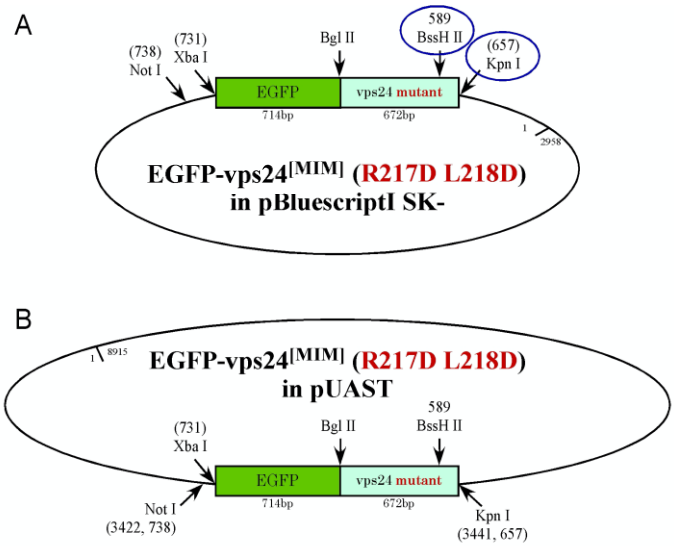

Figure 9. Generation of the EGFP-vps24[MIM] transgene construct in the pUAST vector.

(A) BssH II and Kpn I restriction sites (circled) were used to introduce the PCR fragment containing the R217D and L218D mutations into the wild-type EGFP-vps24 transgene to replace the corresponding wild-type sequence. (B) Not I and Kpn I restriction sites were used to ligate the EGFP-vps24[MIM] sequence into the pUAST transformation vector.

Generation of Transgenic Lines

Generation of the UAS-EGFP-vps24[MIM] transgene construct was completed and transgenic lines were established as described previously and in the Materials and Methods (Chapter 2). Transgene expression levels driven by the neuron-specific Appl-GAL4 driver were assessed in each line by Western blotting. EGFP-VPS24[MIM] expression levels for each line were compared to that of the EGFP-VPS24 transgenic line used in the rescue experiments (Figures 2 and 4). For these experiments, comparable expression levels of the mutant VPS24 fusion protein and the wild-type VPS24 fusion protein is desirable in order to compare their functional defects. An anti-GFP antibody was used to detect expression of the transgene products. The expression level in lines 17B1 and 61A was similar to that of EGFP-VPS24 (Figure 10) and thus these lines were selected for further analysis.

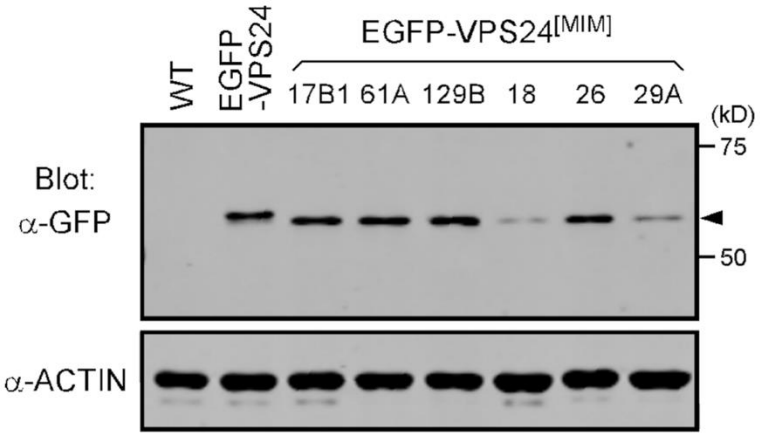

Figure 10. Analysis of transgenic expression levels of individual EGFP-VPS24[MIM] lines.

Western blot analysis of fly head homogenates prepared from WT flies and flies exhibiting neuronal transgenic expression of a fusion protein, EGFP-VPS24, or EGFP-VPS24[MIM]. The mutant VPS24 fusion protein (arrow) migrated at a slightly lower relative molecular mass in comparison to wild-type VPS24 fusion protein. Expression in lines 17B1 and 61A was similar to that of EGFP-VPS24. The bands detected with α-GFP were absent in WT. ACTIN was used as an internal loading control.

Chapter 5

Discussion and Future Directions

Our previous genetic screen revealed a new nonsense mutation in the *Drosophila vps24* gene encoding a component of the ESCRT-III complex, VPS24, which functions in the highly conserved ESCRT pathway. Behavioral testing showed this mutation led to a TS paralytic phenotype. In this mutant, expression of WT VPS24 in neurons yielded rescue of the phenotype. Through the lifespan and climbing analyses described in Chapter 3, the mutation was shown to cause deficiencies in both locomotion and viability. Rescue experiments indicated neuronal expression of WT VPS24 is essential for basic motor function and lifespan. Considering the role of VPS24 in the ESCRT pathway, these results corroborate previous studies linking ESCRT-III components to neurodegenerative disease.

To examine the cellular phenotype of the $vps24^{1}$ mutant, multiple immunocytochemistry experiments were conducted. Ubiquitin-positive structures accumulated in the CNS and DLM of the mutant. Interestingly, the only CNS cell types exhibiting high ubiquitin were neurons. Given the ESCRT pathway's role in lysosomal degradation, as well as prior findings that neurons are less capable of maintaining proteostasis relative to other CNS cell types (Katsuno et al., 2018), these results suggest proteostasis is being negatively impacted by the mutation. To further support this conclusion, additional studies investigated the location of the ubiquitin-positive structures and the mutation's effect on the ESCRT and lysosomal degradation pathways. Colocalization of ubiquitin to LAMP and Cathepsin B verified that the ubiquitin-positive structures were present in expanded lysosomal compartments. Similarly, colocalization of ubiquitin and VPS28, an ESCRT protein that associates with VPS24, in both neurons and muscle suggested the mutant phenotype disrupts ESCRT pathway function. Accumulation of

endogenous P62, an adaptor protein linking ubiquitinated proteins to autophagosome membranes, demonstrated the buildup of autophagic intermediates and, thusly, autophagy disruption in the *vps24*[1] mutant. On the basis of immunocytochemical studies, loss of VPS24 function hinders autophagic degradation and yields undegraded ubiquitinated proteins at the lysosomal compartment. In addition, the observed expanded lysosome might reflect a novel role for VPS24 in either lysosome turnover or formation. A role in turnover would be consistent with ESCRT function in autophagic degradation of lysosomes and the observed accumulation of ubiquitinated proteins. Alternatively, a role in lysosome formation would suggest that loss of VPS24 function leads to accumulation of lysosome intermediates that are arrested during lysosome biogenesis.

TEM was utilized to analyze the ultrastructure of the mutant CNS and DLM. In mutant neurons, cell bodies were enlarged and contained autolysosomes and a prominent tubular lysosomal network, consistent with immunocytochemical evidence of expanded lysosomal compartments. These expanded compartments have not been described in previous ESCRT pathway mutants. Autolysosomes continuous with this network were less electron dense than isolated autolysosomes, suggesting the tubular network is related to tubular intermediates in lysosome biogenesis and providing evidence towards a novel role for the ESCRT pathway in lysosome formation. In muscle, the presence of autophagic intermediates indicated the disruption of autophagy.

To further examine the interaction of VPS24 with ESCRT pathway intermediates, we established transgenic lines expressing the R17D L218D mutant form of VPS24. In ongoing studies, we anticipate its MIM1 domain to be dysfunctional at intermediate membrane-associated stages, where effector proteins execute lysophagy or membrane remodeling of the lysosome. If

VPS24 functions exclusively in lysophagy, intermediates containing EGFP-VPS24$^{[MIM]}$ may be colocalized with P62. A role for VPS24 in lysosome reformation from tubular lysosomes would be indicated if EGFP-VPS24$^{[MIM]}$ distribution resembles that of Clathrin or Dynamin and includes association with buds or neck regions of tubular lysosomes. Future studies will include coimmunoprecipitation studies of EGFP-VPS24$^{[MIM]}$ to identify VPS24-interacting proteins within stalled intermediates.

The results reported in this thesis reveal disruption of lysosome homeostasis and autophagy resulting from loss of VPS24 function. In addition, they suggest that the ESCRT pathway functions in lysosome biogenesis through tubular intermediates. These studies further our understanding of the ESCRT pathway's role in cellular homeostasis and neurodegenerative diseases associated with dysfunctional lysosomal degradation. Improving our grasp of the molecular mechanisms underlying this process may contribute to the design of therapies for NDD patients.

Bibliography

Bajorek, M., Schubert, H. L., Mccullough, J., Langelier, C., Debra, M., Stubblefield, W. B., … Sundquist, W. I. (2009). *Structural Basis for ESCRT-III Protein Autoinhibition*. *16*(7), 754–762. https://doi.org/10.1038/nsmb.1621.Structural

Bjørkøy, G., Lamark, T., Brech, A., Outzen, H., Perander, M., Øvervatn, A., … Johansen, T. (2005). p62/SQSTM1 forms protein aggregates degraded by autophagy and has a protective effect on huntingtin-induced cell death. *Journal of Cell Biology*, *171*(4), 603–614. https://doi.org/10.1083/jcb.200507002

Brand, A. H., & Perrimon, N. (1993). Targeted gene expression as a means of altering cell fates and generating dominant phenotypes. *Development*, *118*(2), 401–415.

Brooks, I. M., Felling, R., Kawasaki, F., & Ordway, R. W. (2003). Genetic analysis of a synaptic calcium channel in Drosophila: Intragenic modifiers of a temperature-sensitive paralytic mutant of cacophony. *Genetics*, *164*(1), 163–171.

Chen, Y., & Yu, L. (2018). Development of research into autophagic lysosome reformation. *Molecules and Cells*, *41*(1), 45–49. https://doi.org/10.14348/molcells.2018.2265

Clague, M. J., & Urbé, S. (2010). Ubiquitin: Same molecule, different degradation pathways. *Cell*, *143*(5), 682–685. https://doi.org/10.1016/j.cell.2010.11.012

Csizmadia, T., Lorincz, P., Hegedus, K., Széplaki, S., Low, P., & Juhász, G. (2018). Molecular mechanisms of developmentally programmed crinophagy in Drosophila. *Journal of Cell Biology*, *217*(1), 361–374. https://doi.org/10.1083/jcb.201702145

Cummings, J. (2017). Disease modification and Neuroprotection in neurodegenerative disorders. *Translational Neurodegeneration*, *6*(1), 1–7. https://doi.org/10.1186/s40035-017-0096-2

Danieli, A., & Martens, S. (2018). P62 - Mediated phase separation at the intersection of the

ubiquitin-Proteasome system and autophagy. *Journal of Cell Science*, *131*(19). https://doi.org/10.1242/jcs.214304

Danjo, R., Kawasaki, F., & Ordway, R. W. (2011). A tripartite synapse model in Drosophila. *PLoS ONE*, *6*(2), 2–7. https://doi.org/10.1371/journal.pone.0017131

Fader, C. M., & Colombo, M. I. (2009). Autophagy and multivesicular bodies: Two closely related partners. *Cell Death and Differentiation*, *16*(1), 70–78. https://doi.org/10.1038/cdd.2008.168

Filimonenko, M., Stuffers, S., Raiborg, C., Yamamoto, A., Malerød, L., Fisher, E. M. C., … Simonsen, A. (2007). Functional multivesicular bodies are required for autophagic clearance of protein aggregates associated with neurodegenerative disease. *Journal of Cell Biology*, *179*(3), 485–500. https://doi.org/10.1083/jcb.200702115

Gal, J., Ström, A. L., Kilty, R., Zhang, F., & Zhu, H. (2007). P62 Accumulates and Enhances Aggregate Formation in Model Systems of Familial Amyotrophic Lateral Sclerosis. *Journal of Biological Chemistry*, *282*(15), 11068–11077. https://doi.org/10.1074/jbc.M608787200

Henne, W. M., Buchkovich, N. J., & Emr, S. D. (2011). The ESCRT Pathway. *Developmental Cell*, *21*(1), 77–91. https://doi.org/10.1016/j.devcel.2011.05.015

Ho, S. N., Hunt, H. D., Horton, R. M., Pullen, J. K., & Pease, L. R. (1989). Site-directed mutagenesis by overlap extension using the polymerase chain reaction. *Gene*, *77*(1), 51–59.

Hung, Y. H., Chen, L. M. W., Yang, J. Y., & Yuan Yang, W. (2013). Spatiotemporally controlled induction of autophagy-mediated lysosome turnover. *Nature Communications*, *4*, 1–7. https://doi.org/10.1038/ncomms3111

Jeibmann, A., & Paulus, W. (2009). Drosophila melanogaster as a model organism of brain diseases. *International Journal of Molecular Sciences*, *10*(2), 407–440.

https://doi.org/10.3390/ijms10020407

Katsuno, M., Sahashi, K., Iguchi, Y., & Hashizume, A. (2018). Preclinical progression of neurodegenerative diseases. *Nagoya Journal of Medical Science*, *80*(3), 289–298. https://doi.org/10.18999/nagjms.80.3.289

Kawasaki, F., Collins, S. C., & Ordway, R. W. (2002). Synaptic calcium-channel function in Drosophila: Analysis and transformation rescue of temperature-sensitive paralytic and lethal mutations of Cacophony. *Journal of Neuroscience*, *22*(14), 5856–5864. https://doi.org/10.1523/jneurosci.22-14-05856.2002

Kawasaki, F., Koonce, N. L., Guo, L., Fatima, S., Qiu, C., Moon, M. T., … Ordway, R. W. (2016). Small heat shock proteins mediate cell-autonomous and -nonautonomous protection in a Drosophila model for environmental-stress-induced degeneration. *DMM Disease Models and Mechanisms*, *9*(9), 953–964. https://doi.org/10.1242/dmm.026385

Kawasaki, F., Mattiuz, A. M., & Ordway, R. W. (1998). Synaptic physiology and ultrastructure in comatose mutants define an in vivo role for NSF in neurotransmitter release. *Journal of Neuroscience*, *18*(24), 10241–10249. https://doi.org/10.1523/jneurosci.18-24-10241.1998

Kawasaki, F., & Ordway, R. W. (2009). Molecular mechanisms determining conserved properties of short-term synaptic depression revealed in NSF and SNAP-25 conditional mutants. *Proceedings of the National Academy of Sciences of the United States of America*, *106*(34), 14658–14663. https://doi.org/10.1073/pnas.0907144106

Leung, K. F., Dacks, J. B., & Field, M. C. (2008). Evolution of the multivesicular body ESCRT machinery; retention across the eukaryotic lineage. *Traffic*, *9*(10), 1698–1716. https://doi.org/10.1111/j.1600-0854.2008.00797.x

Lim, J., & Yue, Z. (2015). Neuronal aggregates: formation, clearance and spreading. *Dev Cell.*,

32(4), 491–501. https://doi.org/10.1016/j.physbeh.2017.03.040

Lloyd, T. E., & Taylor, J. P. (2010). Flightless flies: Drosophila models of neuromuscular disease. *Annals of the New York Academy of Sciences*, *1184*, 1–25. https://doi.org/10.1111/j.1749-6632.2010.05432.x

McCullough, J., Frost, A., & Sundquist, W. I. (2018). Structures, Functions, and Dynamics of ESCRT-III/Vps4 Membrane Remodeling and Fission Complexes. *Annual Review of Cell and Developmental Biology*, *34*(1), 85–109. https://doi.org/10.1146/annurev-cellbio-100616-060600

Muzioł, T., Pineda-Molina, E., Ravelli, R. B., Zamborlini, A., Usami, Y., Göttlinger, H., & Weissenhorn, W. (2006). Structural Basis for Budding by the ESCRT-III Factor CHMP3. *Developmental Cell*, *10*(6), 821–830. https://doi.org/10.1016/j.devcel.2006.03.013

Nagy, P., Varga, Á., Kovács, A. L., Takáts, S., & Juhász, G. (2015). How and why to study autophagy in Drosophila: It's more than just a garbage chute. *Methods*, *75*, 151–161. https://doi.org/10.1016/j.ymeth.2014.11.016

Obita, T., Saksena, S., Ghazi-Tabatabai, S., Gill, D. J., Perisic, O., Emr, S. D., & Williams, R. L. (2007). Structural basis for selective recognition of ESCRT-III by the AAA ATPase Vps4. *Nature*, *449*(7163), 735–739. https://doi.org/10.1038/nature06171

Pandey, U. B., & Nichols, C. D. (2011). Human Disease Models in Drosophila melanogaster and the Role of the Fly in Therapeutic Drug Discovery. *Pharmacological Reviews*, *63*(2), 411–436. https://doi.org/10.1124/pr.110.003293.411

Pankiv, S., Clausen, T. H., Lamark, T., Brech, A., Bruun, J. A., Outzen, H., … Johansen, T. (2007). p62/SQSTM1 binds directly to Atg8/LC3 to facilitate degradation of ubiquitinated protein aggregates by autophagy*[S]. *Journal of Biological Chemistry*, *282*(33), 24131–

24145. https://doi.org/10.1074/jbc.M702824200

Papadopoulos, C., & Meyer, H. (2017). Detection and Clearance of Damaged Lysosomes by the Endo-Lysosomal Damage Response and Lysophagy. *Current Biology*, *27*(24), R1330–R1341. https://doi.org/10.1016/j.cub.2017.11.012

Pulipparacharuvil, S., Akbar, M. A., Ray, S., Sevrioukov, E. A., Haberman, A. S., Rohrer, J., & Krämer, H. (2005). Drosophila Vps16A is required for trafficking to lysosomes and biogenesis of pigment granules. *Journal of Cell Science*, *118*(16), 3663–3673. https://doi.org/10.1242/jcs.02502

Reiter, L. T., Potocki, L., Chien, S., Gribskov, M., & Bier, E. (2001). A systematic analysis of human disease-associated gene sequences in Drosophila melanogaster. *Genome Research*, *11*(6), 1114–1125. https://doi.org/10.1101/gr.169101

Rodríguez-Galán, O., Galindo, A., Hervás-Aguilar, A., Arst, H. N., & Peñalva, M. A. (2009). Physiological involvement in pH signaling of Vps24-mediated recruitment of Aspergillus PalB cysteine protease to ESCRT-III. *Journal of Biological Chemistry*, *284*(7), 4404–4412. https://doi.org/10.1074/jbc.M808645200

Rohrer, J., Schweizer, A., Russell, D., & Kornfeld, S. (1996). The targeting of lamp1 to lysosomes is dependent on the spacing of its cytoplasmic tail tyrosine sorting motif relative to the membrane. *Journal of Cell Biology*, *132*(4), 565–576. https://doi.org/10.1083/jcb.132.4.565

Saffi, G. T., & Botelho, R. J. (2019). Lysosome Fission: Planning for an Exit. *Trends in Cell Biology*, *29*(8), 635–646. https://doi.org/10.1016/j.tcb.2019.05.003

Saftig, P., & Klumperman, J. (2009). Lysosome biogenesis and lysosomal membrane proteins: trafficking meets function. *Nature Reviews Molecular Cell Biology*, *10*(9), 623–635.

https://doi.org/10.1038/nrm2745

Scheffner, M., Nuber, U., & Huibregtse, J. M. (1995). Protein ubiquitination involving an E1–E2–E3 enzyme ubiquitin thioester cascade. *Nature*, *373*(6509), 81–83. https://doi.org/10.1038/373081a0

Shim, S., Kimpler, L. A., & Hanson, P. I. (2007). Structure/function analysis of four core ESCRT-III proteins reveals common regulatory role for extreme C-terminal domain. *Traffic*, *8*(8), 1068–1079. https://doi.org/10.1111/j.1600-0854.2007.00584.x

Stoka, V., Turk, V., & Turk, B. (2016). Lysosomal cathepsins and their regulation in aging and neurodegeneration. *Ageing Research Reviews*, *32*, 22–37. https://doi.org/10.1016/j.arr.2016.04.010

Stuchell-Brereton, M. D., Skalicky, J. J., Kieffer, C., Karren, M. A., Ghaffarian, S., & Sundquist, W. I. (2007). ESCRT-III recognition by VPS4 ATPases. *Nature*, *449*(7163), 740–744. https://doi.org/10.1038/nature06172

Takáts, S., Pircs, K., Nagy, P., Varga, Á., Kárpáti, M., Hegedus, K., … Juhász, G. (2014). Interaction of the HOPS complex with Syntaxin 17 mediates autophagosome clearance in Drosophila. *Molecular Biology of the Cell*, *25*(8), 1338–1354. https://doi.org/10.1091/mbc.E13-08-0449

Taylor, P., Brown, R., & Cleveland, D. (2016). *Neurodegenerative Diseases*. *539*(7628), 179.

Tong, Y., Giaime, E., Yamaguchi, H., Ichimura, T., Liu, Y., Si, H., … Shen, J. (2012). Loss of leucine-rich repeat kinase 2 causes age-dependent bi-phasic alterations of the autophagy pathway. *Molecular Neurodegeneration*, *7*(1), 2. https://doi.org/10.1186/1750-1326-7-2

Veron, J., Kinsella, K., & Velkoff, V. A. (2002). An Aging World: 2001. *International Population Reports*, *57*(6), 928. https://doi.org/10.2307/1534740

Weidberg, H., Shvets, E., & Elazar, Z. (2011). Biogenesis and Cargo Selectivity of Autophagosomes. In *Annual Review of Biochemistry* (Vol. 80, pp. 125–156). https://doi.org/10.1146/annurev-biochem-052709-094552

Wu, Y., Kawasaki, F., & Ordway, R. W. (2005). Properties of short-term synaptic depression at larval neuromuscular synapses in wild-type and temperature-sensitive paralytic mutants of Drosophila. *Journal of Neurophysiology*, *93*(5), 2396–2405. https://doi.org/10.1152/jn.01108.2004

Yu, L., McPhee, C. K., Zheng, L., Mardones, G. A., Rong, Y., Peng, J., … Lenardo, M. J. (2010). Autophagy termination and lysosome reformation regulated by mTOR. *Nature*, *465*(7300), 942–946. https://doi.org/10.1038/nature09076.Autophagy

Yu, S., & Melia, T. (2017). The coordination of membrane fission and fusion at the end of autophagosome maturation. *Curr Opin Cell Biol.*, *47*(1), 92–98. https://doi.org/10.1016/j.physbeh.2017.03.040

Yu, W., Kawasaki, F., & Ordway, R. W. (2011). Activity-dependent interactions of NSF and SNAP at living synapses. *Molecular and Cellular Neuroscience*, *47*(1), 19–27. https://doi.org/10.1016/j.mcn.2011.02.002

ACADEMIC VITA

JONATHAN FLORIAN
jrf5604@psu.edu / jonathan.florian@gmail.com

EDUCATION

2016-2020 The Pennsylvania State University | Schreyer Honors College
Candidate for Bachelor of Science, Biomedical Engineering (Biomaterials)
Date of Graduation: May 2020
Minor: Biology
Area of Honors: Biology

RESEARCH EXPERIENCE

2016-2020 The Pennsylvania State University | Dr. Fumiko Kawasaki & Dr. Richard Ordway
Undergraduate Researcher in Molecular Neuroscience and Genetics
Goal: Study the genetic and environmental factors contributing to neurodegeneration using *Drosophila* as a model organism

- Investigated molecular mechanisms of neurodegeneration in *Drosophila*
- Established and maintained time-sensitive *Drosophila* crosses

Skills obtained: Transgenic line generation, Western blotting, immunocytochemistry, PCR, DNA purification/extraction/digestion, experimental design, genetic analysis, *Drosophila* larval microdissection, laboratory documentation

TEACHING EXPERIENCE

Summer 2018 Teaching Assistant, Cellular and Molecular Neuroscience Laboratory (BIOL 497)
The Pennsylvania State University
Course Instructor: Dr. Fumiko Kawasaki

- Oversaw and advised students performing PCR, genomic prep, and Western blotting
- Explained conceptual and technical details of biology protocols to novices
- Provided feedback on student assignments to reinforce topics and discussions

Summer 2019 Teaching Assistant, Cellular and Molecular Neuroscience Laboratory (BIOL 497)
The Pennsylvania State University
Course Instructor: Dr. Fumiko Kawasaki

HONORS AND AWARDS

2017 Dandrea Trustee Scholarship

2017-2018	John White General Scholarship
2017-2020	Anderson Memorial Scholarship in Engineering
2018-2019	B&P Chapman Trustee Scholarship
2018-2020	Tau Beta Pi Engineering Honor Society
2019	Herbert H. & Beatrice S. Scholarship
2019	T. & B. Pinkerton Open Doors Scholarship
2019-2020	Phi Kappa Phi Honor Society
2019-2020	Academic Excellence Scholarship
2020	S. & T. Ross Trustee Scholarship

SERVICE & LEADERSHIP

2016-2020 Service Vice President, General Member | Penn State Music Service Club

- Provided the elderly and people with disabilities merriment through informal music recitals
- Coordinated with activity directors of LifeLink, CEEL, THON, and the Hershey Medical Center
- Received the Penn State Performing Art Council's Empower the Arts Grant (2019)

2019-2020 General Member | Council of Lionhearts

- Represented the Music Service Club in a campus-wide service organization collaboration
- Deliberated on successful practices promoting member recruitment, retention, and participation
- Pitched discussion strategies to the Music Service Club's executive board